博士学位論文

造影ハーモニック超音波内視鏡検査による胃粘膜下腫瘍の診断における新規腫瘍追跡技術を用いた人工知能の有用性

近畿大学大学院
医学研究科医学系専攻

田　中　秀　和

Doctoral Dissertation

Value of artificial intelligence with novel tumor tracking technology in the diagnosis of gastric submucosal tumors by contrast-enhanced harmonic endoscopic ultrasonography

October 2022

Major in Medical Sciences
Kindai University Graduate School of Medical Sciences

Hidekazu Tanaka

課博

同　意　書

2022 年 10 月 19 日

近畿大学大学院
医学研究科長　殿

共著者 工藤正俊 ㊞　　共著者 大本俊介 ㊞

共著者 渡邉智裕 ㊞　　共著者 三島秀輔 ㊞

共著者 西山直毅 ㊞　　共著者 大塚康生 ㊞

共著者 鎌田研 ㊞　　共著者 吉田晃浩 ㊞

共著者 竹中完 ㊞　　共著者 石川嵐 ㊞

論文題目

Value of artificial intelligence with novel tumor tracking technology in the diagnosis of gastric submucosal tumors by contrast-enhanced harmonic endoscopic ultrasonography

下記の博士論文提出者が、標記論文を貴学医学博士の学位論文（主論文）として使用することに同意いたします。

また、標記論文を再び学位論文として使用しないことを誓約いたします。

記

1．博士論文提出者氏名　　田中　秀和

2．専攻分野　　医学系　　消化器病態制御学

課博

同　意　書

2022　年 10 月 19 日

近畿大学大学院
医学研究科長　殿

共著者 半田久志 ㊞　　共著者 ＿＿＿＿＿＿＿＿ ㊞

共著者 石原里夏 ㊞　　共著者 ＿＿＿＿＿＿＿＿ ㊞

共著者 ＿＿＿＿＿＿＿＿ ㊞　　共著者 ＿＿＿＿＿＿＿＿ ㊞

共著者 ＿＿＿＿＿＿＿＿ ㊞　　共著者 ＿＿＿＿＿＿＿＿ ㊞

共著者 ＿＿＿＿＿＿＿＿ ㊞　　共著者 ＿＿＿＿＿＿＿＿ ㊞

論文題目

Value of artificial intelligence with novel tumor tracking technology in the diagnosis of gastric submucosal tumors by contrast-enhanced harmonic endoscopic ultrasonography

下記の博士論文提出者が、標記論文を貴学医学博士の学位論文（主論文）として使用することに同意いたします。

また、標記論文を再び学位論文として使用しないことを誓約いたします。

記

1．博士論文提出者氏名　　田中　秀和

2．専攻分野　　医学系　　消化器病態制御学

課博

同　意　書

2022 年 10 月 19 日

近畿大学大学院
医学研究科長　殿

共著者	山﨑 友裕 ㊞	共著者	㊞
共著者	山雄 健太郎 ㊞	共著者	㊞
共著者	岡本 彩那 ㊞	共著者	㊞
共著者	吉川 智恵 ㊞	共著者	㊞
共著者	中井 敦史 ㊞	共著者	㊞

論文題目

Value of artificial intelligence with novel tumor tracking technology in the diagnosis of gastric submucosal tumors by contrast-enhanced harmonic endoscopic ultrasonography

下記の博士論文提出者が、標記論文を貴学医学博士の学位論文（主論文）として使用することに同意いたします。

また、標記論文を再び学位論文として使用しないことを誓約いたします。

記

1．博士論文提出者氏名　　田中　秀和

2．専攻分野　　医学系　　消化器病態制御学

近畿大学大学院医学研究科

Value of artificial intelligence with novel tumor tracking technology in the diagnosis of gastric submucosal tumors by contrast-enhanced harmonic endoscopic ultrasonography

Running title: Artificial intelligence and contrast-enhanced endoscopic ultrasonography

Hidekazu Tanaka[1], MD, Ken Kamata[1], MD, PhD, Rika Ishihara[2], ME, Hisashi Handa[2, 3, 4], PhD, Yasuo Otsuka, MD, Akihiro Yoshida[1], MD, Tomoe Yoshikawa[1], MD, Rei Ishikawa[1], MD, PhD, Ayana Okamoto[1], MD, PhD, Tomohiro Yamazaki[1], MD, Atsushi Nakai[1], MD, Shunsuke Omoto[1], MD, PhD, Kosuke Minaga[1], MD, PhD, Kentaro Yamao[1], MD, PhD, Mamoru Takenaka[1], MD, PhD, Tomohiro Watanabe[1], MD, PhD, Naoshi Nishida[1], Masatoshi Kudo[1], MD, PhD

1) Department of Gastroenterology and Hepatology, Kindai University Hospital, Osaka-sayama, Japan

2) Department of Informatics, Kindai University, Higashi-Osaka, Japan

3) Cyber Informatics Research Institute, Kindai University, Higashi-Osaka, Japan

4) Research Institute of Science and Technology, Kindai University, Higashi-Osaka, Japan

Corresponding author: Ken Kamata, MD, PhD

Department of Gastroenterology and Hepatology, Kindai University Faculty of Medicine, 377-2 Ohno-higashi, Osaka-sayama 589-8511, Japan

Tel: +81 72 366 0221 (ext. 3525)

Fax: +81 72 367 2880

E-mail: ky11@leto.eonet.ne.jp

Author contributions:

Hidekazu Tanaka: writing of the manuscript, study conception and design, and blind reading of CH-EUS results. Ken Kamata: writing of the manuscript, study conception and design, and blind reading of CH-EUS results. Rika Ishihara and Hisashi Handa: evaluation of artificial intelligence results and contribution to writing. Yasuo Otsuka, Akihiro Yoshida, Tomoe Yoshikawa, Rei Ishikawa, Ayana Okamoto, Tomohiro Yamazaki, Atsushi Nakai, Shunsuke Omoto, Kosuke Minaga, and Kentaro Yamao: data collection and performance EUS. Mamoru Takenaka, Tomohiro Watanabe, Naoshi Nishida, and Masatoshi Kudo: contribution to writing and revising the manuscript.

Potential competing interests: There are no potential competing interests concerning this study.

Funding information: None

Abbreviations

AI: artificial intelligence

CE-CT: contrast-enhanced computed tomography

CH-EUS: contrast-enhanced harmonic endoscopic ultrasonography

CI: confidence interval

Convnet: convolutional neural network

CT: computed tomography

EUS: endoscopic ultrasonography

EUS-FNA: endoscopic ultrasound-guided fine needle aspiration

GIST: gastrointestinal stromal tumor

g-SMT: gastric submucosal tumor

Resnet: residual neural network

ABSTRACT

BACKGROUND AND AIMS: Contrast-enhanced harmonic endoscopic ultrasonography (CH-EUS) is useful for the diagnosis of lesions inside and outside the digestive tract. This study evaluated the value of artificial intelligence (AI) in the diagnosis of gastric submucosal tumors by CH-EUS.

METHODS: This retrospective study included 53 patients with gastrointestinal stromal tumors (GISTs) and leiomyomas, all of whom underwent CH-EUS between June 2015 and February 2020. A novel technology, SiamMask, was used to track and trim the lesions in CH-EUS videos. CH-EUS was evaluated by AI using deep learning involving a residual neural network and leave-one-out cross-validation. The diagnostic accuracy of AI in discriminating between GISTs and leiomyomas was assessed and compared with that of blind reading by two expert endosonographers.

RESULTS: Of the 53 patients, 42 had GISTs and 11 had leiomyomas. Mean tumor size was 26.4 mm. The consistency rate of the segment range of the tumor image extracted by SiamMask and marked by the endosonographer was 96% with a Dice coefficient. The sensitivity, specificity, and accuracy of AI in diagnosing GIST were 90.5%, 90.9%, and 90.6%, respectively, whereas those of blind reading were 90.5%,

81.8%, and 88.7%, respectively (P = 0.683). The κ-coefficient between the two reviewers was 0.713.

CONCLUSIONS: The diagnostic ability of CH-EUS results evaluated by AI to distinguish between GISTs and leiomyomas was comparable with that of blind reading by expert endosonographers.

Key words: artificial intelligences, contrast-enhanced harmonic endoscopic ultrasonography, gastrointestinal stromal tumor, endoscopic ultrasonography, submucosal tumor, neural network

Introduction

Endoscopic ultrasonography (EUS) is a diagnostic method for the detection and discrimination of gastric submucosal tumors (g-SMTs) [1]. Differential diagnosis of these tumors is challenging because g-SMTs originating from the muscle layer, such as gastrointestinal stromal tumors (GISTs) and leiomyomas, appear similar on EUS [2]. Contrast-enhanced harmonic endoscopic ultrasonography (CH-EUS) enables the qualitative diagnosis of g-SMT by evaluating blood flow [3, 4]. We previously reported the utility of CH-EUS in the differential diagnosis of GISTs and g-SMTs other than GISTs and in the estimation of GIST malignancy [3, 4]. Subjective evaluation of the amount of blood flow, the homogeneity of contrast enhancement, and the morphology of intratumoral blood vessels by more than two experts, however, may lead to diagnostic bias [3-7]. Although EUS-guided tissue sampling is also useful for diagnosing g-SMTs [8], its accuracy can be greatly affected by tumor location and size [5, 6]. Thus, diagnostic imaging still plays a pivotal role in the diagnosis of g-SMTs. Artificial intelligence (AI), a mathematical predictive technique that automates learning and the recognition of data patterns, has been used in the evaluation of endoscopic images [9-13]. SiamMask is a novel tracking and segmentation technology, which enables the position of the tracked object in the video to be estimated and outputs a binary mask indicating the area to which

the object belongs at the pixel level [14]. In the present study, SiamMask was utilized to track and trim lesions in each frame of CH-EUS videos, and the ability of AI using this novel technology to differentiate between GISTs and leiomyomas on CH-EUS was assessed.

Patients and methods

Patients and study design

This was a single-center, retrospective study. The study protocol was approved by the Ethics Committee of Kindai University Faculty of Medicine. The leave-one-out cross-validation method was used for deep learning and diagnosis of AI; therefore, the learning and diagnostic cohorts were not separated. Fifty-three consecutive patients diagnosed with g-SMT by surgical resection or endoscopic ultrasound-guided fine needle aspiration (EUS-FNA) between June 2015 and February 2020 were evaluated. Patients were included if they were aged ≥20 years, had undergone CH-EUS, and had a g-SMT originating from the muscle layer that was diagnosed as GIST or leiomyoma. GIST was defined as a subepithelial tumor composed of spindle cells that stained positive for c-kit and CD34.

Contrast-enhanced harmonic endoscopic ultrasonography

CH-EUS was performed by expert endosonographers (i.e., all had experience of more than 1000 CH-EUS procedures) using a convex type echoendoscope (GF-UCT260; Olympus Medical Systems Co. Ltd., Tokyo, Japan) and imaging equipment (ALOKA ProSound SSD α-10 or F75 system; ALOKA Co. Ltd., Tokyo, Japan). The transmitting frequency and mechanical index were 4.7MHz and 0.3, respectively. Patients received the ultrasound contrast agent Sonazoid (Daiichi-Sankyo, Tokyo, Japan) at a concentration of 0.015 mL/kg body weight and underwent CH-EUS examination under conscious sedation with propofol. CH-EUS videos were stored in a recording system, with videos taken approximately 20 seconds after blood flow was first observed in the tumor evaluated by blinded readers and AI. For blind reading, the enhancement patterns of the lesions were divided into hyper- and hypo-enhancement, as described [3]. Hyper-enhanced lesions were considered to be GISTs whereas hypo-enhanced lesions were considered to be leiomyomas. The stored data were reviewed by two experienced readers (H. Tanaka and K. Kamata), who were blinded to the clinical findings, with any differences resolved by consensus re-reading.

SiamMask

SiamMask is a metric learning approach, utilized to track objects in each frame image in movies. Images in the first and subsequent frames are defined as the target and search images, respectively [15-19]. The region of the tracking object in the target image is initially set manually, with regions in search images estimated by SiamMask. This estimation process is iterative, with the search image in each iteration becoming the target image in the next iteration. Thus, manually setting the region of the tracking object is only required in the initial iteration [20]. AI trimming of the tumor area in EUS videos has also been found useful [21].

The process from input to output of the tumor image by SiamMask is illustrated in Figure 1. The search image and the cropped local image are passed through the same network (f_θ), with each feature map obtained by the residual neural network (Resnet) (i.e., Resnet50). The feature map of the local image is subsequently subjected to 2D convolution performed (*d), with each spatial element (response of a candidate window) yielding two interrelated feature maps (response maps). Similarity, bounding box coordinates and a value mask are generated; the output of the three branches consists of two 1x1 convolution layers ($h\varnothing$, $b\delta$, $s\varphi$) generated by the convolutional neural network (CNN; convnet) [14]. After applying sigmoid to each pixel, the output of the mask branch is digitized with a threshold of 0.5. For frames other than the first frame, the output mask

was fit with a min-max box, which was used as a reference for the search area of the next frame. An image was created in which only the tumor part was removed from the search image and the value mask. Figure 2 shows a representative image, in which both the tumor area extracted by SiamMask and manually marked by the endosonographer are shown in white and the rest of the background in black. The consistency rate of the segment range of the tumor obtained by those two methods was 96% with a Dice coefficient [22]. Thus, SiamMask trimmed the tumor area of the first image and automatically tracked the tumor in the CH-EUS video (Video 1).

Deep learning and diagnosis by artificial intelligence

Deep learning and diagnosis by AI included feature extraction, classification, and probabilistic distribution processes (Figure 3). A 20-second CH-EUS video from each patient was divided into 0.1 second intervals, yielding 200 images. Features were extracted from each image using SiamMask as described above. For classification, the images extracted by SiamMask were converted to 256 × 256 pixels images and labeled as “GIST” or “Leiomyoma”; these images were used for training Resnet. The output of Resnet was based on SoftMax, which provides estimates for GIST ranging from 0 to 1.0.

After deep learning using data other than those of the target patient, the values of the 200 images obtained from the target patient were estimated and averaged to obtain the final result; this was done using the learn-one-out cross validation method. Thus, data from 52 enrolled patients, excluding the target patient, were used as training data. This process was repeated for all 53 enrolled patients. If AI estimated "GIST" with a probability ≥0.5, it was considered to be “GIST”.

Statistical analysis

The rate of consistency of the segment range of the tumor images extracted by SiamMask and marked by the endosonographer was compared by determining Dice coefficients. The accuracy of diagnosis of GIST by blind reading and AI was compared using the McNemar test. Interobserver agreement in CH-EUS findings was tested by kappa statistics, with κ coefficients of > 0.8, > 0.6, and > 0.4 indicating excellent, good, and moderate agreement, respectively. All statistical analyses were performed using SAS software version 9.1 (SAS Institute, Cary, NC, USA), with P values <0.005 considered statistically significant.

Results

Fifty-three patients, 28 men and 25 women (mean age, 64.4 years) were eligible for analysis (Table 1). Of these patients, 42 were diagnosed with GIST and 11 with leiomyoma. Mean tumor size was 26.4 mm. The consistency rate between the segment range of the tumor image extracted by SiamMask and that marked by the endosonographer was 96%. The κ-coefficient between the two reviewers was 0.713. Overall, sensitivity, specificity, and accuracy of AI for diagnosing GIST were 90.5%, 90.9%, and 90.6%, respectively, whereas those for blind reading were 90.5%, 81.8%, and 88.7%, respectively (Table 2). The difference was not significant (P = 0.683). The diagnostic performance of AI and blind reading was in perfect agreement for cases with a tumor < 20mm (n = 17); and showed a trend similar to that observed for the entire in cases with tumors 20 mm ≥ (n = 36).

There were few tumors with probability values of around 0.5, indicating that AI clearly distinguished between GISTs and leiomyomas (Table 3). Video 2 shows the CH-EUS of a patient with GIST (patient 2 in Table 3). Blind reading found hypo-enhancement, indicating leiomyoma, whereas AI estimated the probability of GIST at 86%. Video 3 shows the CH-EUS of a patient with a leiomyoma (patient 23 in Table 3). Blind reading found hyper-enhancement indicating GIST, whereas AI estimated the probability of GIST at 6%.

Discussion

AI is being developed as a new diagnostic tool for endoscopy. In gastrointestinal endoscopy, AI has been used in the diagnosis of gastric cancers, colorectal polyps, and intraductal papillary mucinous neoplasms [10, 23, 24]. This study examined the diagnostic ability of AI with CH-EUS for g-SMTs. AI systems using deep learning methods such as convnet have been developed in several fields. CNNs have proven effective models for a variety of visual tasks, resulting in several high-performance algorithms, such as AlexNet [25], GoogleNet [26], VGG16 [27], YOLO [28], and Resnet [10]. Resnet is composed of residual blocks, with shortcut connections between CNN layers. The present study used the Resnet algorithm for marking tumors and diagnosing gastric SMTs.

SiamMask is an AI method of tracking tumors on CH-EUS videos in real time and trimming tumor images using Resnet. The present study compared tumor images marked by SiamMask and by endosonographers, finding a 96% concordance rate in the Dice coefficient and indicating that SiamMask is considered useful for marking. Traditionally, video images are individualized, with marked tumors or images saved at the time of examination. Isolating the tumor area on saved images using SiamMask allowed more

images to be obtained over a short time and improved work efficiency. Using saved videos, it should be possible to create AI learning data and perform diagnoses in an almost fully automatic manner.

A meta-analysis found that the pooled sensitivity, specificity, and accuracy of CH-EUS for discriminating between GIST and benign SMT were 89%, 82%, and 89%, respectively [29]. Few studies, however, have evaluated the ability of CH-EUS to diagnose g-SMTs [29, 30], and its diagnostic performance has been found to vary [30]. In the present study, evaluation of CH-EUS findings by blinded readers had a sensitivity, specificity, and accuracy of 90.5%, 81.8%, and 88.7%, respectively. Thus, the diagnostic performance was comparable with that of the above meta-analysis.

A comparison of the diagnostic ability of expert endosonographers and AI to distinguish between GISTs and leiomyomas revealed no significant differences ($P = 0.683$). However, AI showed greater specificity than the expert endosonographers. In some cases, it may be difficult to differentiate GISTs from leiomyomas based on subjective evaluation of contrast patterns alone. In several patients, the AI diagnosis was correct, whereas the diagnosis by the endosonographers was incorrect. Correct diagnosis of these patients required endosonographers to learn the key findings of AI. Although checking AI heat maps is important, it is difficult to determine the criteria used by AI to make a diagnosis

due to the wide range of variations in each heat map image. This might be solved in the future by accumulating data from a large number of patients. Minoda, et al. reported the usefulness of conventional EUS using AI for SMT; however, there are several differences between that study and our own (other than not using CH-EUS) [11]. In that study, the training and validation were performed using separate data sets. The final diagnosis for the training data was based only on EUS-guided sampling. Various types of EUS, including convex and radial type EUS and EUS prove, were used. Also, EUS imaging equipment from a different company was used. Finally, 15–20 conventional EUS images per patient were used for diagnosis [11].

The present study had several limitations, including its retrospective design and its inclusion of a relatively small number of patients. The EUS videos were collected retrospectively, which may have led to selection bias. The gold standard is EUS-FNA and surgery, and there were only two cases with resected leiomyoma in our cohort. However, differential diagnosis of benign and malignant g-SMT has improved with the advancement of diagnostic imaging and EUS-guided sampling methods and the number of surgical cases with leiomyoma is not expected to increase. The test data were verified using the leave-one-out cross validation method. The use of different processors (ALOKA

ProSound SSD α-10 or F75 system) may have led to a different interpretation by AI, although settings such as frequency and mechanical index were consistent.

In conclusion, automatic segmentation of g-SMT lesions using SiamMask reduces the effort associated with traditional manual labor in AI-based diagnostic imaging. Moreover, AI with novel tumor tracking technology may be useful for the differential diagnosis of GISTs and leiomyomas by CH-EUS.

References

1. Akahoshi K, Oya M, Koga T et al. Current clinical management of gastrointestinal stromal tumor. World journal of gastroenterology 2018; 24: 2806-2817.
2. Nishida T, Hirota S. Biological and clinical review of stromal tumors in the gastrointestinal tract. Histology and histopathology 2000; 15: 1293-1301.
3. Kamata K, Takenaka M, Kitano M et al. Contrast-enhanced harmonic endoscopic ultrasonography for differential diagnosis of submucosal tumors of the upper gastrointestinal tract. Journal of gastroenterology and hepatology 2017; 32: 1686-1692.
4. Sakamoto H, Kitano M, Matsui S et al. Estimation of malignant potential of GI stromal tumors by contrast-enhanced harmonic EUS (with videos). Gastrointestinal endoscopy 2011; 73: 227-237.
5. Akahoshi K, Oya M, Koga T et al. Clinical usefulness of endoscopic ultrasound-guided fine needle aspiration for gastric subepithelial lesions smaller than 2 cm. Journal of gastrointestinal and liver diseases 2014; 23: 405-412.
6. Sepe PS, Moparty B, Pitman MB et al. EUS-guided FNA for the diagnosis of GI stromal cell tumors: sensitivity and cytologic yield. Gastrointestinal endoscopy 2009; 70: 254-261.
7. Yang YT, Shen N, Ao F et al. Diagnostic value of contrast-enhanced harmonic endoscopic ultrasonography in predicting the malignancy potential of submucosal tumors: a systematic review and meta-analysis. Surgical endoscopy 2020; 34: 3754-3765.
8. Kamata K, Kurita A, Yasukawa S et al. Utility of a 20G needle with a core trap in EUS-guided fine-needle biopsy for gastric submucosal tumors: A multicentric prospective trial. Endoscopic ultrasound 2021; 10: 134-140.
9. Kuwahara T, Hara K, Mizuno N et al. Current status of artificial intelligence analysis for endoscopic ultrasonography. Digestive endoscopy 2021; 33: 298-305.
10. Kuwahara T, Hara K, Mizuno N et al. Usefulness of Deep Learning Analysis for the Diagnosis of Malignancy in Intraductal Papillary Mucinous Neoplasms of the Pancreas. Clinical and translational gastroenterology 2019; 10: 1-8.
11. Minoda Y, Ihara E, Komori K et al. Efficacy of endoscopic ultrasound with artificial intelligence for the diagnosis of gastrointestinal stromal tumors. Journal of gastroenterology 2020; 55: 1119-1126.

12. Xia J, Xia T, Pan J et al. Use of artificial intelligence for detection of gastric lesions by magnetically controlled capsule endoscopy. Gastrointestinal endoscopy 2021; 93: 133-139.
13. He YS, Su JR, Li Z et al. Application of artificial intelligence in gastrointestinal endoscopy. Journal of digestive diseases 2019; 20: 623-630.
14. Q. Wang LZ, L. Bertinetto, et al. Fast Online Object Tracking and Segmentation: A Unifying Approach. IEEE/CVF Conference on Computer Vision and Pattern Recognition (CVPR) 2019.
15. Santoro A, Bartunov S, Botvinick M et al. Meta-learning with memory-augmented neural networks. International conference on machine learning. PMLR 2016: 1842-1850.
16. Vanschoren J. Meta-learning. Automated Machine Learning. Springer, Cham 2019: 35-61.
17. Timothy Hospedales AA, Paul Micaelli, Amos Storkey. Meta-Learning in Neural Networks: A Survey. ArXiv 2020.
18. Hospedales T, Antoniou A, Micaelli P et al. Meta-learning in neural networks: A survey. ArXiv 2020.
19. O Vinyals CB, T Lillicrap, K Kavukcuoglu et al.. Matching Networks for One Shot Learning. Proceedings of the 30th International Conference on Neural Information Processing SystemsDecember 2016; 3637-3645.
20. Z. Liang CL, Y. Zhang, H. Mu et al. Tracking of Moving Target Based on SiamMask for Video SAR System. IEEE International Conference on Signal, Information and Data Processing (ICSIDP) 2019; 1-4.
21. Iwasa Y, Iwashita T, Takeuchi Y, et.al. Automatic Segmentation of Pancreatic Tumors Using Deep Learning on a Video Image of Contrast-Enhanced Endoscopic Ultrasound. J Clin Med 2021; 10: 3589.
22. Jha D, Smedsrud PH, Riegler MA et al. Resunet++: An advanced architecture for medical image segmentation. IEEE International Symposium on Multimedia (ISM) 2019: 225-2255.
23. Hirasawa T, Aoyama K, Tanimoto T et al. Application of artificial intelligence using a convolutional neural network for detecting gastric cancer in endoscopic images. International Gastric Cancer Association and the Japanese Gastric Cancer Association 2018; 21: 653-660.
24. Komeda Y, Handa H, Watanabe T et al. Computer-Aided Diagnosis Based on Convolutional Neural Network System for Colorectal Polyp Classification: Preliminary Experience. Oncology 2017; 93: 30-34.

25. Krizhevsky A. SI, Hinton G. ImageNet classification with deep convolutional neural networks. Adv Neural Inf Process Syst 2012; 25: 1097–1105.
26. Szegedy C. LW, Jia Y, et al. Going deeper with convolutions. ArXiv 2014; 1409: 4842.
27. He K. ZX, Ren, et al. Deep residual learning for image recognition.preprint ArXiv 2015; 1512: 3385.
28. Redmon J DS, Girshick R, Farhadi A. You only look once: Unified, real-time object detection. IEEE Conference on Computer Vision and Pattern Recognition (CVPR) 2016: 779-788.
29. Tang JY, Tao KG, Zhang LY et al. Value of contrast-enhanced harmonic endoscopic ultrasonography in differentiating between gastrointestinal stromal tumors: A meta-analysis. Journal of digestive diseases 2019; 20: 127-134.
30. Kitano M, Yamashita Y, Kamata K et al. The Asian Federation of Societies for Ultrasound in Medicine and Biology (AFSUMB) Guidelines for Contrast-Enhanced Endoscopic Ultrasound. Ultrasound in medicine & biology 2021; 47: 1433-1447.

Figure legends

Figure 1. Illustration of the SiamMask process, from input to output of tumor images.

Figure 2. Results from a representative patient, showing the tumor area (A) extracted by SiamMask (B) and marked manually by the endosonographer (C).

Figure 3. Illustration of the extraction, classification, and probabilistic distribution processes in deep learning and diagnosis.

Video legends

Video 1. CH-EUS video, showing trimming of the tumor area of the first image and automatic tracking of the tumor by SiamMask.

Video 2. CH-EUS video of a GIST correctly diagnosed by AI but incorrectly diagnosed by blind reading.

Video 3. CH-EUS video of a leiomyoma correctly diagnosed by AI but incorrectly diagnosed by blind reading.

Table1. Patient characteristics

Total	n=53
Mean age, y (range)	64.4 (20–90)
Male/Female, n	28/25
GIST/Leiomyoma	42/11
Mean tumor size, mean ± SD, mm	26.4 ± 12.9
Tumor location (Fundus/ Cardia/Antrum/Body)	10/7/5/31
Final diagnosis (Surgical resection/ EUS-FNA)	33/20

Abbreviations: EUS-FNA, endoscopic ultrasound-guided fine needle aspiration; GIST, gastrointestinal stromal tumor; SD, standard deviation.

Table 2. Diagnosis ability (blind reading vs. AI)

Overall (n = 53)					
	Sensitivity (%)	Specificity (%)	PPV (%)	NPV (%)	Accuracy (%)
Blind reading	90.5	81.8	95.0	69.2	88.7
(95% CI)	(84.2–93.7)	(57.8–94.2)	(88.4–98.4)	(48.9–79.7)	(78.7–93.8)
AI	90.5	90.9	97.4	71.4	90.6
(95% CI)	(84.4–92.4)	(67.9–98.3)	(90.9–99.5)	(53.3–77.2)	(81.0–93.6)
Cases < 20mm (n = 17)					
	Sensitivity (%)	Specificity (%)	PPV (%)	NPV (%)	Accuracy (%)
Blind reading	92.9	100	100	75.0	94.1
(95% CI)	(82.5–92.9)	(51.7–100)	(88.9–100)	(38.8–75.0)	(77.1–94.1)
AI	92.9	100	100	75.0	94.1
(95% CI)	(82.5–92.9)	(51.7–100)	(88.9–100)	(38.8–75.0)	(77.1–94.1)
Cases ≥ 20mm (n = 36)					
	Sensitivity (%)	Specificity (%)	PPV (%)	NPV (%)	Accuracy (%)
Blind reading	89.3	75.0	92.6	66.7	86.1
(95% CI)	(81.1–94.0)	(46.4–91.4)	(84.1–97.5)	(41.3–81.3)	(73.4–93.4)
AI	89.3	87.5	96.2	70.0	88.9
(95% CI)	(81.2–92.2)	(59.2–97.6)	(87.5–99.3)	(47.4–78.1)	(76.3–93.4)

Abbreviations: AI, artificial intelligence; CI, confidence interval; NPV, negative predictive value; PPV, positive predictive value.

Table 3. Final diagnosis and result of AI for each patient

Patient no.	Final diagnosis	Estimated probability of GIST	Patient no.	Final diagnosis	Estimated probability of GIST
1	GIST	0.99	28	Leiomyoma	0.38
2	GIST	0.86	29	GIST	0.97
3	Leiomyoma	0.87	30	GIST	0.73
4	GIST	0.99	31	Leiomyoma	0.02
5	GIST	0.99	32	GIST	0.73
6	Leiomyoma	0.00	33	GIST	0.31
7	GIST	0.84	34	GIST	1.00
8	GIST	1.00	35	GIST	1.00
9	Leiomyoma	0.00	36	GIST	0.62
10	GIST	0.46	37	Leiomyoma	0.06
11	Leiomyoma	0.02	38	GIST	1.00
12	GIST	0.86	39	GIST	0.67
13	GIST	0.98	40	GIST	0.99
14	GIST	0.99	41	GIST	0.98
15	GIST	0.97	42	GIST	0.95
16	Leiomyoma	0.02	43	GIST	0.85
17	GIST	0.98	44	GIST	0.99
18	GIST	1.00	45	Leiomyoma	0.14
19	Leiomyoma	0.05	46	GIST	0.93
20	GIST	0.88	47	GIST	0.94
21	GIST	0.99	48	GIST	0.97
22	GIST	0.02	49	GIST	1.00
23	Leiomyoma	0.06	50	GIST	0.90
24	GIST	1.00	51	GIST	0.99
25	GIST	1.00	52	GIST	0.92
26	GIST	0.32	53	GIST	1.00
27	GIST	1.00			

Abbreviations: GIST, gastrointestinal stromal tumor.

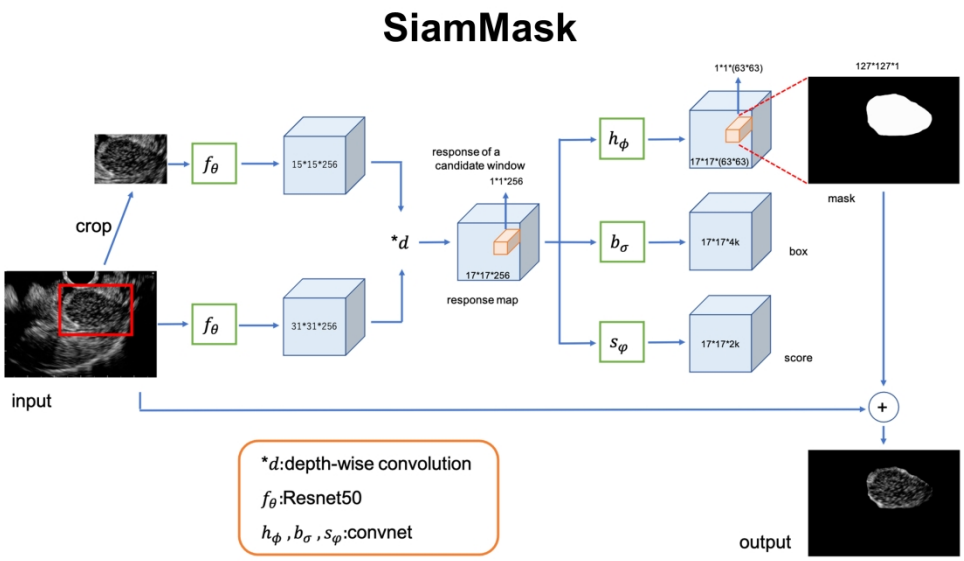

Figure 1. Illustration of the SiamMask process, from input to output of tumor images.

Figure 2. Results from a representative patient, showing the tumor area (A) extracted by SiamMask (B) and manually marked by the endosonographer (C).

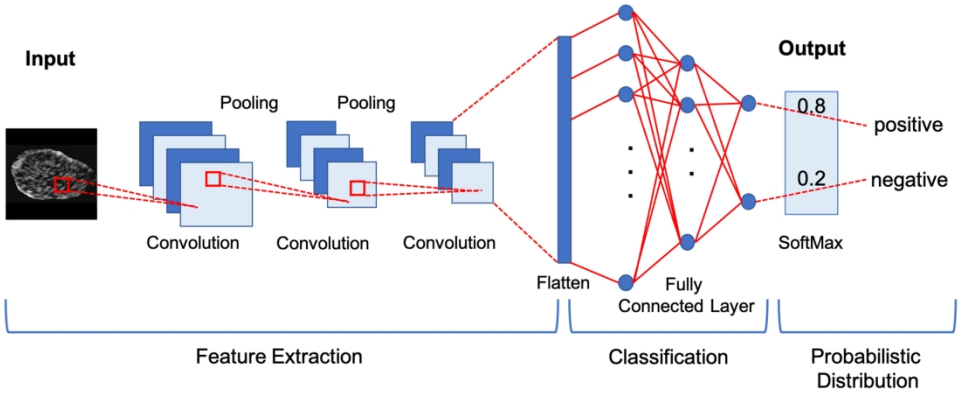

Figure 3. Illustration of the extraction, classification, and probabilistic distribution processes in deep learning and diagnosis.

（謝辞）
今回の研究を進めるに際して、多くの諸先生がたにご指導ご鞭撻を賜りました。
指導教官である近畿大学消化器内科学工藤正俊主任教授からは研究のデザインから実施、評価、論文化まで多岐に渡りご指導を賜り、感謝の念に堪えません。ありがとうございました。
消化器内科学鎌田研講師からは豊富な知識と経験の下、適切なご助言を頂き研究において立ち行かない状態にならずに終了することができました。深く感謝申し上げます。
近畿大学情報学部情報学科半田久志教授には AI や SiamMask の診断プログラムを始め、実際の解析まで施行頂きました。教授の御指導がなければ今回の研究は成立しないものでした。深く感謝申し上げます。
今回の研究を通じて胆膵領域での AI 診断の発展の可能性を見出すことができました。今後も引き続き臨床研究に携わって参りたいと思っております